Performance of a micro-fabricated Colloid thruster system

IEPC-2009- 189

Presented at the 31st International Electric Propulsion Conference,
University of Michigan • Ann Arbor, Michigan • USA
September 20 – 24, 2009

Katharine L. Smith [1] and John P. W. Stark.[2]
Queen Mary University of London, London E1 4NS, United Kingdom

Renato Krpoun [3]
CSEM Brazil, Belo Horizonte, Minas Gerais, 30.170-020, Brazil

and

Herbert Shea [4]
EPFL, Sch Engn, Microsyst Space Technol Lab, CH-2002 Neuchatel, Switzerland

In order to fully characterize the performance of the colloid thruster system the electrospray (ES) beam must itself be fully characterized. This may be achieved by measuring various properties such as flow rate, current, droplet/ion charge to mass ratio and current profile. Beam properties of both standard electrospray mass spectrometry (ESMS) emitters and arrays of custom made micro-fabricated emitters have been determined. By varying the geometries of the micro-fabricated emitters two basic modes of thruster operation have been identified a high Isp with lower thrust density and a lower Isp with higher thrust density. The versatility of this system allows for a thruster design that has a thrust range spanning two orders of magnitude from ~ 5 to 500μN with highly competitive power requirements ~ 0.05W/μN. The proposed thruster system is designed to meet the needs of future formation flying missions.

Nomenclature

L	=	beam flight path for TOF
$\dot{m}$	=	mass flow rate
q/m	=	charge to mass ratio
Q	=	volumetric flow rate
V_{acc}	=	applied voltage to acceleration grid
V_{em}	=	applied voltage to emitter (submerged counter electrode)
V_{ext}	=	applied voltage to extraction grid
V_T	=	total acceleration potential

[1] Lecturer, School of Engineering and Materials Science, k.smith@qmul.ac.uk.
[2] Professor and Head of School, School of Engineering and Materials Science, j.p.w.stark@qmul.ac.uk.
[3] Project Manager , Centro de Inovações CSEM Brasil, renato.krpoun@csembrasil.com.br.
[4] Professor, School of Engineering, Microsystems Space Technology Lab, herbert.shea@epfl.ch.

I. Introduction

The fundamental advantages of electric propulsion have already been successfully applied to a variety of applications including Telecommunication Satellites (ARTEMIS/ALPHABUS), Earth Observation (GOCE) and Science Spacecraft (SMART-1/BepiColombo). Concerns about global warming and climate change have resulted in a growing requirement to measure the Earth's upper atmosphere on a regular basis. The instruments for such missions, Lidars and cloud measuring radar, function most effectively at low altitudes. To achieve stable positioning of a Spacecraft at these altitudes, low thrust electric propulsion is required to compensate for the atmospheric drag effect and to provide fine attitude control. Another emerging market need is the exploitation of large distributed aperture instruments through precision formation flying [1-4]. Missions such as Proba 3, PRISMA and LISA Pathfinder are planned to help demonstrate formation flying technologies for future scientific missions such as LISA, DARWIN and Xeus.

In order to respond to the specific propulsion and control needs of these missions, alternative micro-propulsion technologies are required. These technologies must be scalable and flexible in order to provide a relatively wide range of thrusts for the different mission scenarios, and must have very low thrust resolutions and low thrust noise to meet attitude control and payload requirements.

The colloid thruster has been identified as a candidate technology for on-board micro-propulsion for future scientific, small telecommunication and earth observation satellites together with formation flying missions[5]. These missions are generally achieved at low thrust levels however mass constraints require relatively high specific impulses, with low power availability. The core design principle of a colloid thruster is the use of an electrospray (ES) to generate a beam of charged droplets, which are then accelerated in a static electric field. In order to fully characterize the performance of the colloid thruster system the ES beam must itself be fully characterized. This may be achieved by measuring various properties such as flow rate, current, droplet/ion charge to mass ratio and beam charge density profile.

In this paper beam properties of both standard electrospray mass spectrometry (ESMS) emitters and arrays of custom made micro-fabricated emitters are presented. Time of flight (TOF) techniques coupled with mass flow rate measurements were used to determine charge to mass ratio distribution. Beam angle was also determined from beam charge density decay measurements.

Two basic modes of thruster operation have been identified a high Isp with lower thrust density and a lower Isp with higher thrust density. We have also identified that both these modes may be attained on a similar MEMS chip by tuning the hydraulic impedance of individual emitters[6]. The versatility of this system allows for a thruster design that has a thrust range spanning two orders of magnitude from ~ 5 to 500μN with highly competitive power requirements ~ 0.05W/μN. This range of thrust has been identified as that required to meet the needs of future formation flying missions[7].

II. Experimental Configurations

Two sets of tests were carried out in order to determine the overall performance of the proposed colloid thruster system. Initial beam characterization of the ionic liquid EMI-BF_4 tests from a single 30μm standard ESMS emitter with a single extraction grid. Further testing of integrated emitter array and extraction grid with an additional acceleration grid was used to demonstrate functionality and performance of these devices.

The Emitters used for the single grid initial beam characterization tests were 30μm Silica Tips from New Objective. These emitters have a tip dimensional accuracy of +/- 2μm. The New Objective emitters were mounted directly into a fluid reservoir that was placed inside the vacuum test chamber. The fluid reservoir was manufactured from the vacuum compatible polymer PEEK. A submerged counter electrode consisted of a sleeve of stainless steel press fit into the internal bore of the PEEK fluid reservoir. This stainless steel insert provided electrical contact between the high voltage power supply (HVPS) and the fluid in the reservoir. A schematic of the TOF system used in the single emitter single grid tests is shown in Figure 1. For the beam angle measurements the TOF target was replaced by a moveable segmented target.

The second test configuration was to test the performance of a breadboard model of a hybrid colloid thruster system, shown in Figure 2, incorporating a 19-emitter micro-fabricated (MEMS) emitter-extractor system (from EPFL) with a conventionally fabricated fluid reservoir and acceleration grid. The fluid reservoir was similar to the one used in the initial testing of the standard ESMS emitters. A modified TOF configuration was used to test the EPFL emitters; this modified configuration avoids the issue of turning on and off the emitter source by employing an electrostatic gate. A schematic of this TOF configuration is shown in Figure 3.

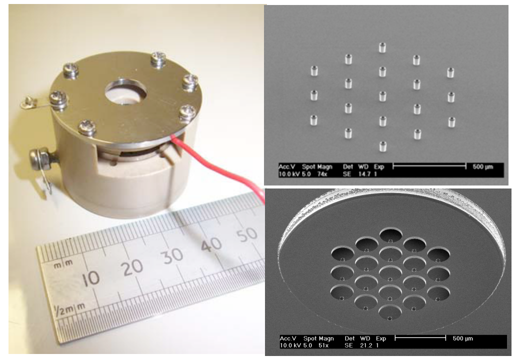

Figure 2. Hybrid Colloid Thruster system.

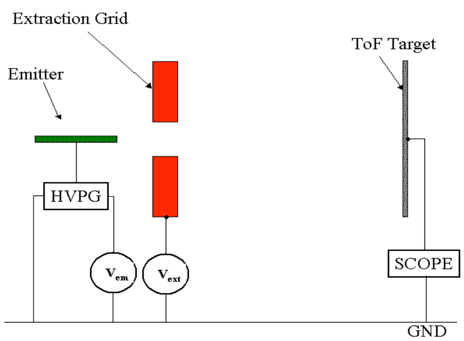

Figure 1. System configuration for single grid tests New Objective emitter.

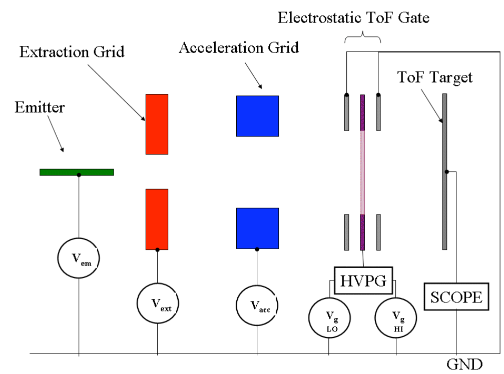

Figure 3. Schematic of TOF configuration for EPFL emitters.

A. TOF for single emitter single grid

TOF traces are essentially the decay current measured on a flat plate collector which is placed downstream of a charged particle source (or 'beam'). By interrupting the beam source this decay current is generated. In the case of the TOF traces produced for the single grid tests, interruption of the applied field, and hence the beam, was achieved by coupling the high voltage power supply used to generate the static field with a high speed pulse generator (capable of generating high voltage pulses with decay times ~6ns). The resulting decay currents measured on the downstream collector were then used to determine the average velocity and charge of the charged components of the beam.

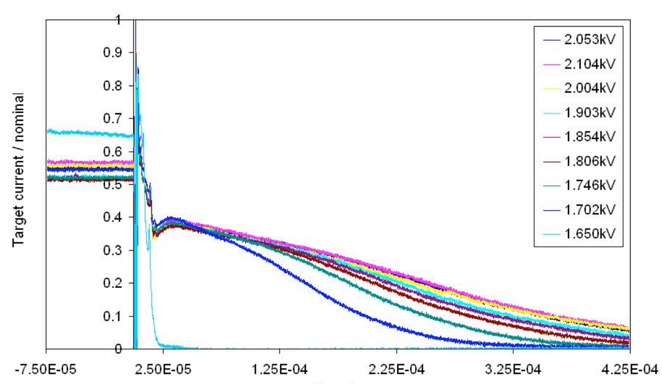

Figure 4. TOF traces for EMI-BF$_4$ sprayed from a 30µm New Objective emitter for a range of extraction potentials.

TOF traces for EMI-BF$_4$ sprayed from a 30µm New Objective emitter for a range of extraction potentials are shown in Figure 4. The TOF traces in Figure 4 illustrate the nature of the EMI-BF$_4$ beam from a 30µm emitter, it can be seen from these traces that the beam is ~ 30% ions (the short timescale spike) with a large (~70% beam) droplet tail. A close up of the ion portion a TOF trace is shown in Figure 4. This illustrates that three distinct ion species are present in the beam with varying proportions of these species depending on extraction potential. Figure 5 also illustrates that the electrospray conditions can be set so that the beam is purely ionic i.e. that only monomer, dimmer and trimer species are present in the beam, this is seen for the 1.650kV case.

The mass flow rate may be determined from the time of flight traces using the equation

$$\dot{m} = 4\frac{2V_T}{L^2}\int_0^{\infty} I t dt \qquad (1)$$

Where L is the length of the flight path of the charged particles and V_T is the total acceleration potential. Equation 1 has been used to determine the mass flow rate for each TOF spectra at a given potential.

The average charge to mass ratio at each extraction potential may be independently evaluated simply from the ratio of the total emitted charge and the mass flow rate. Figure 6 shows a plot of this average charge to mass ratio as a function of volumetric flow rate for data obtained under atmospheric conditions and vacuum conditions. For the data obtained at atmospheric pressure measurement of the flow rate was made using the flow meter system previously reported [8-10]. Also shown in Figure 6 are experimentally obtained data for the same ionic liquid (EMI-BF_4) reported by Romero-Sanz [11]. It is clear that both the vacuum data and the air data we have obtained are broadly consistent with Romero-Sanz's data.

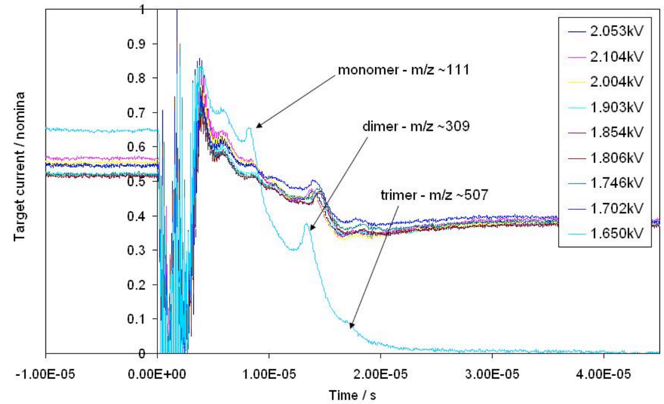

Figure 5. Close up of ion portion of TOF traces for EMI-BF_4 sprayed from a 30µm New Objective emitter for a range of extraction potentials

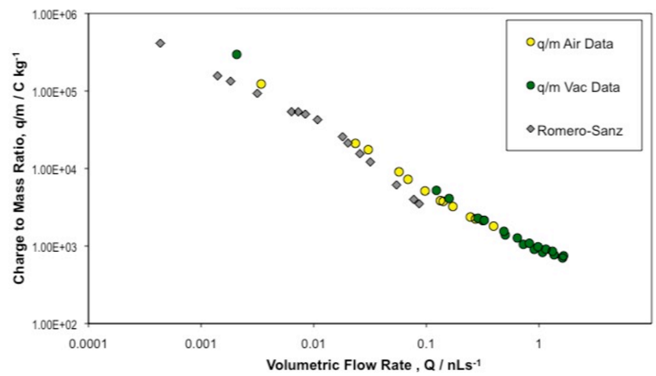

Figure 6. Single grid average charge to mass ratio vs. flow rate.

B. Beam angle estimation

The beam geometry was defined by using a segmented electrode, similar to that used in [12, 13], to determine the current measured in concentric circular electrodes, centered on the beam centre line. Beam profiles were obtained at three downstream locations at distances of 75 mm, 150 mm and 410mm from the emitter source. The current density as a function of radial location is shown for each downstream position in Figure 7. From this figure it is apparent that both as a function of downstream distance these profiles were flat across the beam suggesting that the beam species/energy composition is uniform, and the beam is well mixed at these downstream locations. Similar flat beam profiles have been observed by other researchers in the field [13]. In order to achieve such a distribution it may be assumed that the species profile across the beam is well mixed at the distances along the beam for which these measurements were obtained.

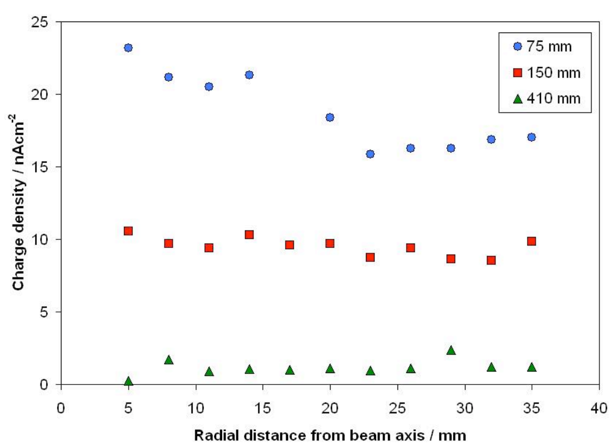

Figure 7. Charge density of the Beam as a function of position from beam centre for three different downstream

The overall beam decay properties are shown in Figure 8. The beam charge density decay data has been used to estimate the beam radius as function of axial location in order to identify the beam spread angle. From this analysis we conclude from the three points that the beam spread angle is ~20°.

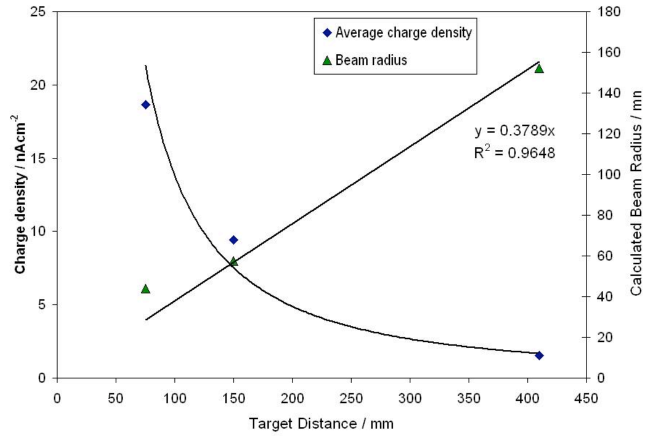

Figure 8. Single Grid Beam radius derived from beam

C. TOF results for Hybrid Colloid Thruster system (with EPFL 19 emitter array)

The MEMS emitters used in this study were micro-fabricated using a deep reactive ion etching (DRIE) process as described in refs [14-16]. In addition to this DRIE manufacturing process the hydraulic impedance of the emitters was modified by filling with silica microspheres, a process which is described in ref [17]. The results presented here are from these 'filled' emitters only. The geometry of each emitter was similar to that of the New Objective standard ESMS used in the previously described tests, however the extraction electrode was placed much closer to enable much lower extraction potentials.

An initial back pressure of ~200mbar was required to initiate spraying as a result of the system hydraulic impedance. Once the array was spraying the emitter voltage V_{em} was ramped from 0.7 – 1.4 kV while the extractor voltage, V_{ext} and acceleration voltage V_{acc} were kept fixed at ground potential. Figure 9 shows the TOF traces obtained from this test. It is clear from Figure 9 that the beam is highly ionic throughout the entire voltage range with an increasing monomer component with increasing V_{em}. Another interesting point to note from Figure 9 is the small cluster/droplet component at the lower voltages. It may be concluded from these observations that due to the high fluidic impedance of the emitter capillaries, due to their partial filling with 5micron silicon beads, the spray is initially in the pulsating mode with a small droplet component. As the field strength increases and the stress on the fluid surface increases the spray enters a purely ionic mode where a dual-energetic beam eventually gives way to a mono-energetic beam with further increase in applied field. We have observed such behavior previously from very narrow bore capillaries without the addition of flow impedance devices.

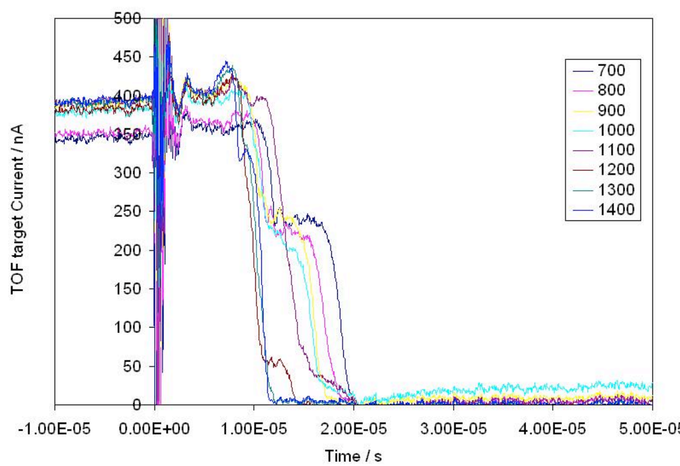

Figure 9. TOF trace from 19 emitter EPFL array.

The continued increase in voltage does not result in the system entering the droplet (high thrust, low Isp) mode. This is believed to arise simply because continued electrical stressing of the fluid by electric pressure alone is unable to raise the flow rate sufficiently.

D. Thruster design ethos

From the single emitter and 19 emitter array tests described in this paper we have identified two basic modes of thruster operation, namely; a high Isp low thrust density mode (exhibited by the emitters with high hydraulic impedance) and a low Isp high thrust density mode (exhibited by the lower hydraulic impedance 'open' New Objective emitters). Both modes are potentially achievable using a similar emitter design with an additional modification for the higher Isp mode. It is thus envisioned that a segmented thrust head could easily be manufactured that could incorporate separately addressable regions that would satisfy the range of thrust levels required for a variety of future formation flying and other low thrust long duration missions. From the data we have obtained and summarized here, a suitable configuration to demonstrate the feasibility of a throttle able colloid thruster system is detailed in Table 1.

	Low Thrust High Isp Segment	High Thrust Low Isp Segment	
Thrust range [μN]	0-25	50	442
Specific Impulse, I_{sp} [s]	7570	635	1178
Power [W]	0.93	0.25	1.95
# of Emitters	550	194	

Table 1. Proposed Thruster Flight Experiment

III. Conclusions

A hybrid colloid thruster system has been evaluated using experimentally obtained data for both MEMS emitters and standard off the shelf ESMS emitters. Included in this evaluation was the testing of a breadboard model thrust head and fluid reservoir. Two distinct modes of operation were identified; a high thrust low Isp mode and a lower thrust higher Isp mode. Further testing of the breadboard model to include direct thrust measurements is required. However, from the data presented in this paper we have determined a suitable configuration to demonstrate the feasibility of a colloid thruster package capable of meeting the station keeping and low thrust requirements for a range of future missions. The principal specifications of this system are a throttleable thrust of 0 to ~500μN with a specific power of 6 to 37W/mN.

Acknowledgments
The authors would like to thank Dr. Clive Edwards for his continued support throughout this study and the European Space Agency (ESA) for providing the funds necessary to continue this work.

References

1. ESA, *CDF Study Report Proba 3 Formation Flight Technology Demonstrator and Coronagraph Mission*. 2005, ESA. p. CDF-42(A).
2. ESA, *Darwin TTN+ Mission Design Assessment*. 2004, ESA. p. SCI-A/2004/187/Darwin/DMS.
3. ESA, *LISA - System and Technology Study Report*. 2000. p. ESA-SCI(2000)11v1.05.
4. ESA, *CDF Study Report XEUS X-ray evolving universe spectroscopy*. 2004. p. CDF-31(A).
5. Zeimer, J. and S.M. Merkowitz, *NASA Microthruster Developments*, in *5th International LISA Symposium*. 2004, NASA JPL: Montana.
6. Krpoun, R., et al., *Tailoring the hydraulic impedance of out-of-plane micromachined electrospray sources with integrated electrodes.* Applied Physics Letters, 2009. **94**(16): p. 163502.
7. ESA, *Proba 3 Preliminary Electric Propulsion System Requirements*. 2007. p. P3-EST-RS-3001 Draft 2.
8. Smith, K.L., *Characterisation of electrospray properties in high vacuum with a view to application in colloid thruster technology*, in *Engineering*. 2005, Queen Mary University of London: London.

9. Smith, K.L., M.S. Alexander, and J.P.W. Stark, *Voltage effects on the volumetric flow rate in cone-jet mode electrospraying.* Journal of Applied Physics, 2006. **99**: p. 064909.
10. Smith, K.L., M.S. Alexander, and J.P.W. Stark, *The Sensitivity of Volumetric Flow Rate to Applied Voltage in Cone-Jet Mode Electrospray and the Influence of Solution Properties and Emitter Geometry.* Physics of Fluids, 2006. **18**: p. 092104.
11. Romero-Sanz, I., et al., *Source of heavy molecular ions based on Taylor cones of ionic liquids operating in the pure ion evaporation regime.* Journal of Applied Physics, 2003. **94**: p. 3599.
12. Lozano, P., *Studies on the Ion-Droplet Mixed Regime in Colloid Thrusters*, *MIT Thesis*, M. Martinez-Sanchez, Editor. 2003.
13. Lozano, P. and M. Martinez-Sanchez, *Jets and Sprays Emitted from Colloid Thrusters -Experiments and Modeling.* Proceedings 3rd International Conference on Spacecraft Propulsion, 2000. **ESA SP -465**: p. 451.
14. Krpoun, R., M. Raber, and H.R. Shea, *Microfabrication and test of an integrated colloid thruster.* Mems 2008: 21st Ieee International Conference on Micro Electro Mechanical Systems, Technical Digest, 2008: p. 964-967.
15. Krpoun, R., et al. *Design and fabrication of an integrated MEMS-based colloid micropropulsion system*. in *30th International Electric Propulsion Conference*. 2007. Florence, Italy: IEPC-2007-099.
16. Krpoun, R. and H.R. Shea, *Integrated out-of-plane nanoelectrospray thruster arrays for spacecraft propulsion.* Journal of Micromechanics and Microengineering, 2009. **19**(4).
17. Krpoun, R., et al., *Tailoring the hydraulic impedance of out-of-plane micromachined electrospray sources with integrated electrodes.* Applied Physics Letters, 2009. **94**(16).